Mosquera Giovanny (Orcid ID: 0000-0002-4764-4685)
Páez-Bimos Sebastián (Orcid ID: 0000-0003-4833-3923)
Crespo Patricio (Orcid ID: 0000-0001-5126-0687)

Delineation of water flow paths in a tropical Andean headwater catchment with deep soils and permeable bedrock

Braulio Lahuatte[1,2], Giovanny M. Mosquera[3,*], Sebastián Páez-Bimos[4,5], Marlon Calispa[6,7], Veerle Vanacker[4], Xavier Zapata-Ríos [5], Teresa Muñoz[8], Patricio Crespo[2]

[1] Fondo para la Protección del Agua de Quito – FONAG, Av. Mariana de Jesús, Quito, 170519, Ecuador.

[2] Departamento de Recursos Hídricos y Ciencias Ambientales, Facultad de Ingeniería & Facultad de Ciencias Químicas, Universidad de Cuenca, Av. 12 de abril, Cuenca, 010150, Ecuador.

[3] Instituto Biósfera, Universidad San Francisco de Quito USFQ, Diego de Robles y Vía Interoceánica, Quito, Ecuador.

[4] George Lemaître Center for Earth and Climate Research, Earth and Life Institute, UCLouvain, Louvain-la-Neuve, Belgium.

[5] Departamento de Ingeniería Civil y Ambiental, Facultad de Ingeniería Civil y Ambiental, Escuela Politécnica Nacional, Quito, Ecuador.

[6] Earth and Life Institute, Environmental Sciences, Université catholique de Louvain, Place Pasteur, 1348 Louvain-la-Neuve, Belgium..

[7] Programa para el Manejo de Agua y Suelo (PROMAS), Facultad de Ingeniería Civil, Universidad de Cuenca, Cuenca, Ecuador.

[8] Empresa Pública Metropolitana de Agua Potable y Saneamiento (EPMAPS), Quito, Ecuador.

*Corresponding authors: Giovanny M. Mosquera (giovamosquera@gmail.com,

gmosquera@usfq.edu.ec)

Keywords: stables isotopes, flow path, runoff generation, Andes, Tropical mountains, Ecuador, Antisana.

Running title: Subsurface water flow paths in young volcanic ash soils

ABSTRACT

Traditional hydrometric data combined with environmental tracers such as water stable isotopes contributes to improve the understanding of catchment hydrology. Nevertheless, the application of isotopic tracers in headwater catchments of the tropical Andes with deep soils and permeable parent material influenced by recent volcanism remains limited. In this study, the stable isotopic composition of precipitation, soil water, wetlands, and streamflow was studied to provide insights into the hydrology of a small tropical Andean catchment with deep and permeable volcanic soils, ash layers, and fractured bedrock resulting from Holocene volcanic activity. Although local precipitation forms under isotopic equilibrium conditions, the stable isotopic composition of precipitation is influenced by atmospheric moisture recycling processes. The spatial and temporal variability of isotopic signals and the analysis of inverse transit time proxies (ITTPs) of surface (streamflow) and subsurface (soil and wetlands) waters indicate that vertical flow paths through the deep volcanic ash soils are dominant across the catchment. The strongly damped isotopic composition of these waters points to high soil and wetlands water storage, increasing the transit time or age of stream water in the hydrological system. These findings indicate that water mobilizing through subsurface flow paths – i.e., volcanic soils, ash layers, and cracks in the fractured bedrock resulting from Holocene volcanism – is the main contributor to streamflow generation. Comparison with previously published work from Andean catchments and other volcanic areas shows the diversity of hydrological conditions that can be found as a result of pedological and lithological differences shaped by volcanic activity. Therefore, site-specific strategies may be needed to improve water resources management.

1. INTRODUCTION

Headwater catchments influenced by volcanism in the tropical Andes provide many ecosystem services including erosion control, carbon sequestration, nutrient cycling, food provisioning, and production of high-quality water (Aparecido et al., 2017; Wright et al., 2017, Mosquera et al., 2021). The latter is favored by relatively low physical erosion rates (i.e., below 30 t km^{-2} yr^{-1}, Tenorio et al. 2018, Vanacker et al., 2022) and sustained rainfall input throughout the year, often presenting no rain periods shorter than two weeks (Célleri et al., 2007), in combination with unique properties of soils formed from volcanic ash accumulation such as high organic matter content (i.e., up to above 53.6%, Nierop et al., 2007; Molina et al., 2019), and high water retention and infiltration capacities (Buytaert et al., 2005, Mosquera et al., 2020b). This water resource is crucial to support the development of urban centers such as Mérida, Bogotá, Cuenca, and Quito (Buytaert & Bièvre, 2012). These cities satisfy their hydroelectric, irrigation, domestic, and industrial needs by using water originated in tropical alpine (páramo) headwater catchments (Célleri & Feyen, 2009).

Despite the importance of volcanic activity in the tropical Andes, surface and subsurface hydrology of catchments in the region are not thoroughly understood. Through the sole use of traditional hydrometric measurements, Ochoa-Tocachi et al. (2016) analyzed the hydrological dynamics of catchments across the tropical Andes and made evidence of the high variability that exists in streamflow response. A systematic review by Mosquera et al (2021) recently highlighted the lack of hydrological knowledge in understudied regions across the tropical Andes such as those dominated by deep ashfall deposits and fractured bedrock resulting from recent volcanism. These studies emphasized the importance of obtaining improved process-based understanding of subsurface flow dynamics. Natural tracers such as water stable isotopes have proven to be useful for catchment hydrology (Kendall & McDonnell, 1998; Leibundgut et al., 2009). The determination of the local meteoric water line (LMWL, i.e., the linear regression between the stable isotopes of hydrogen, δ^2H, and oxygen, $\delta^{18}O$ in local precipitation) allowed Esquivel-Hernández et al. (2019) and Windhorst et al. (2013) to infer processes that control precipitation formation in the highlands of the tropical Andes. The LMWL slope and intercept can show if evaporation plays a major role in the hydrology of surface water bodies (Brooks et al., 2012; Landwehr and Coplen, 2004). In tropical regions, the isotopic composition of precipitation, surface, and subsurface waters has been used to delineate water flow paths in headwater catchments (Crespo et al., 2011; Minaya et al., 2016; Mosquera et al., 2016a; Muñoz-Villers et al., 2016), to quantify water storage (Lazo et al., 2019), and develop conceptual models of catchment hydrological behavior (Mosquera et al., 2020a). Notably, Mosquera et al (2016a) highlighted the value of water stable isotopes to understand hydrological processes of tropical Andean catchments in relatively short time periods (1-2 years), making these tracers a particularly powerful tool to fill key hydrological knowledge gaps in remote regions where monitoring is scarce.

These studies of water mixing processes commonly assume that the isotopic composition of precipitation is conserved as water travels through the system (Kim & Jung, 2014; Oshun et al., 2015). Subsurface movement of the water through internal catchment flow paths causes attenuation of the precipitation signal due to advection and dispersion processes. When the tracer leaves the system through an outflow (e.g., soil water, wetland, or streamflow), it has been affected by these processes and therefore its signal is assumed to reflect the subsurface hydrological dynamics occurring within a catchment (Hrachowitz et al., 2016; Kirchner, 2016; McGuire & McDonnell, 2006). In this sense, inverse transit time proxies (ITTPs, Tetzlaff et al., 2009) have been used to identify differences in internal flow paths of water through the attenuation of the isotopic composition of an outflow in relation to that of precipitation, i.e., the stronger the attenuation, the lower the ITTP and the longer the mean transit time (MTT) or the age of the water. For instance, for montane catchments in the Scottish highlands, Tetzlaff et al. (2009) found that ITTPs of 0.5 to 0.6 corresponded to MTTs of around 4 months, ITTPs of 0.2 to 0.3 corresponded to MTTs of 6 to 12 months, and ITTPs lower than 0.1 corresponded to MTTs of 1 to 3.5 years. The application of water stable isotopes is still limited in the tropical Andes mainly due to the scarcity of isotopic monitoring networks (Mosquera et al., 2016a). In the region, isotopic studies have been predominantly carried out in southern Ecuador (e.g., Correa et al., 2017; Mosquera et al., 2016b; Mosquera et al., 2020a; Ramón et al., 2021), where volcanic soils with shallow depth to the weathered bedrock with very low permeability are dominant (Molina et al., 2019). There exist only few tracer studies in tropical Andean catchments with Holocene volcanic activity, where deep volcanic ash soils are abundant (Tonneijck et al., 2008; Hall et al., 2017). For example, Minaya et al. (2016) studied the role of glacier melting in runoff generation. Nevertheless, process-based understanding of catchment hydrology in these hydrological systems is still missing (Vanacker et al., 2018)

The limited understanding of hydrological processes in catchments with Holocene volcanic activity, such as the ones found in the northern Ecuadorian Andes, is a hindrance to adequate catchment management strategies. A thorough understanding of the catchment hydrology across spatial and temporal scales is key to support water management institutions with ground-based scientific evidence (EPMAPS & FONAG, 2018). The study was conducted in a high-elevation tropical Andean catchment characterized by Holocene volcanic activity and deep volcanic ash soils. This headwater catchment is one of the main water sources of the capital of Ecuador, Quito. Through the use of water stable isotopic tracers, this study seeks to address the following research questions: (i) What are the spatial and temporal patterns of the isotopic composition of surface (streamflow) and subsurface (soil and wetlands) water in relation to precipitation in a small tropical Andean headwater catchment? and (ii) How does water mix at the catchment scale?

2. MATERIALS AND METHODS

2.1 Study Area

This research was developed in a small headwater catchment situated within the Jatunhuaycu Experimental Observatory (JEO, 0°30′19″S, 78°14′29″W; Fig. 1 a,b). The observatory covers an area of 32.6 km^2 of tropical alpine ecosystem (páramo) and used to be part of a cattle farm until 2011 (EPMAPS & FONAG, 2018). The observatory is located in the northern Ecuadorian Andes, specifically within the Antisana Water Conservation Area which is 55 km southeast of Quito city. At the moment, Quito´s Water Fund (FONAG), and Quito´s Metropolitan Drinking Water and Sanitation Company (EPMAPS-Q) own the observatory and are studying its hydrology, ecology, and the impacts of conservation efforts in collaboration with academic partner institutions. The study catchment feeds into the Mica water system, an important water source for EPMAPS-Q and Quito inhabitants (EPMAPS & FONAG, 2018). This study was carried out in a 0.68 km^2 subcatchment, hereafter referred to as JTU_01 (Fig. 1c). JTU_01 was equipped in the scope of the ParamoSUS project, a joint collaboration effort between Ecuadorian and Belgian academic institutions, EPMAPS-Q, and FONAG.

Over the period 2014 to 2021, JTU_01 had a mean annual precipitation of 789 ± 117 mm/year considering that the hydrological year starts in March to coincide with the beginning of the rainy season in the area (Torres & Proaño, 2018). Presenting a relatively small variation (764-887 mm/year), except in the year 2015 when it rained approximately 250 mm less than the average (i.e., 547 mm/year). Thus, precipitation during the monitored period (March 2019 to February 2020; 887 mm/year) is representative for the period 2014 to 2021. Rainfall seasonality during the study period 2014-2021 was low according to the seasonality index (Walsh & Lawler, 1981) that varied between 0.17 and 0.31. For the meteorological station located in the center of the study area, we measured for the period 2019-2021 the following mean annual values: rainfall of 797 ± 129 mm, air temperature of 4.2 ± 0.2 °C, relative humidity of 93.5 ± 0.6 %, incoming short-wave solar radiation of 154 ± 5.8 W m^{-2}, and wind speed of 3.2 ± 0.4 m s^{-1} with dominant wind from east to west throughout the year (Paez-Bimos et al., 2022a). Mean annual discharge during the period 2014-2021 was 82 ± 21 mm/year, presenting a runoff coefficient (ratio of annual discharge to precipitation) below 0.10 (Ochoa-Tocachi et al., 2016). Low runoff coefficients are not unusual in regions with recent or active volcanism that are characterized by deep and permeable volcanic ash layers (Hall et al., 2017), where deep percolation can be important.

Soils near Antisana volcano reach depths of 5 to 7 m and show a sequence of buried soils. In nearby areas, buried soils have been observed at depths of up to 27 meters beneath scoria and glacio-fluvial sediments (Hall et al., 2017). The soils across JTU_01 are young and slightly altered vitric Andosols (Calispa et al., 2021), which developed from ashfall deposits and pyroclastic material from Quilotoa and Cotopaxi volcanos that fell in the area around 800 to 1100 years ago (Onderet, 2018; Hall et al., 2017). Histosols are commonly found in flat zones where organic matter is accumulated (Onderet, 2018). These soils are common in the Andean wetlands and are typically situated at toeslope positions (e.g., Mosquera et al. 2015; Buytaert et al. 2007). Both soil types have high water regulation and retention capacity, low bulk density, and high saturated hydraulic conductivity (Páez-Bimos et al., 2022; Páez-Bimos et al., 2021). The area was affected by intensive cattle and sheep grazing until 2011, and grazing and burning resulted in short-turf grasslands replacing much of the tall-tussock grassland (Grubb et al., 2020). Since then, livestock was excluded, and passive restoration is ongoing. The vegetation distribution is as follows: tussock grass 48%, cushion plants 40%, and others including shrubs and stagnant water bodies 12% (EPMAPS & FONAG, 2018).

2.2 Experimental Design

To better understand the subsurface hydrological behavior in young volcanic ash soils, two experimental hillslopes at JTU_01 were implemented and monitored. The experimental setup at JTU_01 is presented in Fig. 1c. The monitored hillslopes differed only in their dominant vegetation cover. One was dominated by tussock grasses (*Calamagrostis intermedia*) and the other by cushion plants (*Azorella pedunculata*). Hereafter, we will refer to them as TU and CU, respectively. Each hillslope consisted of four soil water sampling positions, upper (UP), upper replica (UR), middle (MI), and lower (LO) (Páez-Bimos et al., 2022a). Wells were installed to monitor the wetlands located at the bottom of each hillslope. These wells consisted of 2 m long PVC pipes of 5 cm diameter that were placed vertically within the wetland. Holes were drilled along the whole length of the pipes every 10 cm to allow soil water to recharge the wells, and a nylon fabric was placed to protect the holes from obstructions. Because of logistic constraints, the TU well was installed at the toe slope position (see contour lines in Fig. 1c), and may be positioned at the transition between hillslope and wetland. A v-notch weir was constructed at the catchment outlet to measure streamflow. Water level data at the weir was monitored every 5 minutes since 2014 using an INW- PT2X water pressure sensor. Discharge was measured using the constant rate salt dissolution technique (Moore, 2005).

Discharge measurements were used to develop a rating curve that was further used to obtain a continuous discharge time series. A TEXAS TR-525M rain gauge and a self-made precipitation water sampler were installed at the upper part of the CU hillslope (Fig. 1c). The rain gauge was used to measure rainfall amount every 5-minutes during the study period. Soil water samplers were also placed at the 8 sampling sites along the experimental hillslopes. The depth of the samplers is presented in Table 1. At each sampling position, the soils were described up to a depth of 135 cm following the FAO (2015) guidelines. Calispa et al (2021) determined five soil horizons, namely O, A, 2A, 2BC, 3BC whereof the isotopic composition of soil water in the A, 2A, 2BC, and 3BC horizons was monitored.

2.3 Collection of water samples

Biweekly samples of precipitation, soil water, wetlands, and streamflow were collected during the period March 2019 to March 2020 (Páez-Bimos et al., 2021). Precipitation samples were obtained using a polypropylene collector covered with aluminum foil. A 5 mm thick oil layer was added into the collector to prevent isotopic fractionation due to evaporation (Mook, 2000). Soil water samples were collected using two types of samplers: ceramic suction cups (SC) and fiber glass wick samplers (WS). SCs were used in the A, 2A, 2BC, and 3BC horizons (Fig. 1c and Table 2). SCs are lysimeters that consist of three parts: the suction cup itself, the sampling bottle, and the suction container. The SCs were 0.50 m in length and had a ceramic cup with a maximum pore size of 1 μm. During each sampling campaign, a negative pressure between 45 to 50 KPa was applied to the SCs to collect soil water into a 500 ml glass bottle. A hose was connected to the glass bottles, covered with aluminum foil, and placed inside closed buckets. WSs were used to collect water in the transition horizons (A-2A, and 2A-2BC). The samplers consisted of 30x30 cm polypropylene plates in which 9.5 mm diameter fiberglass wicks were untangled following the design of Singh et al. (2018). The wicks were placed in direct contact with the soil by digging a hole within the soil pit at the depth of interest. To ensure that the plate was in contact with the soil matrix a press was used to tighten the sampler in the dug hole. A 2-inch PVC tube connected the bottom of the plates with a 1-gallon plastic container. A suction of 55 cm (5.4 KPa) was applied to the wicks following Singh et al. (2018). The codification of soil water samplers includes information about the hillslope dominant vegetation cover (TU or CU), sampling position (UP, UR, MI, or LO), soil water sampling device (SC or WS), and soil horizon or transition (1 for shallow, 2 for intermediate, and 3 for deep). For example, TU-UP-SC1 corresponds to the suction cup (SC) placed in the tussock hillslope (TU), upper position (UP), and in the A horizon (shallowest soil horizon) (Table 2 and Fig. 1c). Accordingly, CU-LO-WS1 corresponds to the wick sampler placed in the cushion hillslope, lower position, and the transition between the A to 2A horizons (first transition, Table 2 and Fig. 1c).

The wetlands (WE) were sampled directly from the wells at the bottom of each hillslope and streamflow (Q) before the v-notch weir. All water samples were filtered using 0.45 μm pore membrane filters (mixed ester of cellulose S-PAK) and stored in 2 ml amber glass bottles. Parafilm was used to reduce evaporation effects on the water samples. Samples were transported and stored without being exposed to light to prevent isotopic fractionation due to evaporation (Mook, 2000).

2.4 Laboratory Analysis

Stable isotopic compositions (δ^2H and $\delta^{18}O$) were determined using a Picarro L2130-i isotope water vapor analyzer with a precision of 0.5‰ for δ^2H and 0.1‰ for $\delta^{18}O$ at the University of Cuenca´s Soil and Water Quality Laboratory. Three secondary standards were used to calibrate the Picarro instrument and ensure analysis quality. To diminish memory effects, the samples were analyzed by batches containing similar water types, and during each analysis, six injections were done into the analyzer and the first three were discarded. The maximum difference of the isotopic values of the last three injections were compared to the equipment precision and the secondary standards´ standard deviation. If such difference was higher than the analytical precision for a given sample, the analysis of that sample was repeated. ChemCorrect 1.2.0 software was used to verify if organic contamination occurred. Only one soil water sample was contaminated, representing 0.08% of all analyzed samples. The results are presented in δ notation using the Vienna-Standard Mean Ocean Water (V-SMOW) as reference (Craig, 1961).

2.5 Spatial and temporal variation of isotopic signal and water mixing analysis

To assess the temporal variation of the stable isotopic composition of precipitation, we evaluated how it varied in relation to precipitation amount. We applied a simple linear regression between δ^2H and $\delta^{18}O$ in precipitation water to determine the LMWL. The LMWL was used as reference for the analysis of fractionation and possible moisture sources coming to the study area by comparing the regression coefficients to those of the global meteoric water line (GMWL, i.e., the linear regression between the stable isotopes of hydrogen, δ^2H, and oxygen, $\delta^{18}O$ in global precipitation, Craig, 1961). In addition, we visually assessed the influence that precipitation isotopic composition had in soil water, wetlands, and streamflow. Specifically, we evaluated if enriched or depleted precipitation influenced the isotopic composition of the surface and subsurface water samples to infer water transport and mixing processes.

Line-conditioned excess (lc-excess, Landwehr & Coplen, 2004) was calculated for soil water, wetlands, and streamflow using the following equation: lc-excess = δ^2H - a×$\delta^{18}O$ - b, where a and b are the LMWL's slope and intercept, respectively. Negative lc-excess values are indicative of post-rainfall evaporative isotopic fractionation (Kendall & Coplen, 2001), whereas positive lc-excess values suggest differences in moisture sources contributing to local precipitation (Landwehr & Coplen, 2004).

In addition, ITTPs were calculated to identify potential differences in subsurface water flow paths and mixing processes (Tetzlaff et al., 2009). The ITTP is a metric of tracer signal damping, which is here calculated as the ratio between the standard deviation of $\delta^{18}O$ in one of the measurements points (e.g., water from soils, wetlands, and streamflow) to the standard deviation of $\delta^{18}O$ in precipitation. We present results based on the $\delta^{18}O$ isotopic composition only, since isotopic fractionation due to evaporation is marginal (see section 4.2), and therefore δ^2H yields the same findings. The standard deviation was derived from all samples collected during the study period.

3. RESULTS

3.1 Precipitation isotopic composition

During the study period, the precipitation regime was bimodal with two precipitation peaks (Fig. 2a). The first rainy season started in March 2019 and finalized in June 2019. A dry season lasting from July to September 2019 followed. A second wet season occurred between October 2019 and March 2020, although two short dry periods (about 2 weeks each) were observed (late January and mid February 2020; Fig. 2a). The temporal variation in precipitation isotopic composition mimicked the temporal fluctuation in precipitation amount, showing depleted isotopic values (<-15‰ in $\delta^{18}O$) during the wettest periods (e.g., Mar-Jun 2019 and Oct 2019) and enriched isotopic values (> -10‰ in $\delta^{18}O$) during the driest periods (e.g., Jun-Sep 2019 and Jan 2020). Figure 2b shows that the $\delta^{18}O$-δ^2H relation in local precipitation (i.e., LMWL) had a similar slope (8.2) than the GMWL (8.0), indicating that evaporation does not affect the isotopic composition of local precipitation (Kendall & McDonnell, 1998). The intercept (*d-excess*) of the LMWL was higher (16.15) than that of the GMWL (10.0), indicating the potential contribution of reevaporated moisture sources to local precipitation (Esquivel-Hernández et al., 2019; Mosquera et al., 2016a; Zhiña et al., 2022).

3.2 Soil water, wetlands, and streamflow isotopic composition

The isotopic composition of soil water, wetlands, and streamflow showed that all samples lie within or very close to the LMWL (Fig 3). These observations depict that they are composed of a mixture of precipitation from different rainfall events. The TU-UR-SC1 and TU-UR-WS1 sampling sites registered the most depleted isotopic compositions (Fig. 3g and Fig. 4a). With regard to enriched values, none of the samples had compositions higher than -10.6‰ in $\delta^{18}O$ and -77‰ in $\delta^{2}H$ (Fig. 3 and Fig. 4a-c). A slight shift was observed in soil water under cushion forming plants, wetlands, and streamflow. Those samples consistently plotted slightly below the LMWL (Fig. 3f-j), while soil water under tussock grasses plotted closer to it. lc-excess values for soil water under cushion forming plants were lower than those in the soils underlying tussock grasses regardless of sampling position and depth (Fig. 4d-f). lc-excess values in most soil water sampling sites were negative with only few samples in the TU soils being positive (Fig. 4d-f). The fact that most surface and subsurface water samples laid very close to the LMWL and lc-excess values were rarely lower than -7.5 indicates that evaporative fractionation can be considered to be marginal in the study area. As both isotopes provide similar information, we show and report only results for $\delta^{18}O$ in the remaining sections.

Figure 5 shows the temporal dynamics of soil water isotopic composition for the different soil water samplers. The attenuation of the isotopic composition of soil water tends to increase as the sampling depth increased (i.e., from Fig. 5 a,b to Fig. 5 i,j). The comparison of the isotopic composition of precipitation and soil water provided some insights into water mixing in the soil. In general, the isotopic composition of soil water in the upper samplers (SC1 and WS1) followed the composition of precipitation at all sampling positions (Fig. 5a, Fig. 5d). For instance, the depleted isotopic composition of rainfall during the first rainy period (March to June 2019) caused a depletion in the isotopic composition of soil water a few biweeks later. This is particularly noticeable for CU-SC1 and TU-WS1, and less evident in CU-WS1 and TU-SC1 (Fig. 5b, c). Slightly enriched isotopic values were found at all positions, except at UR, in the TU-SC1 samplers at the end of the first rainy season (Fig. 5b) when depleted isotopic values were observed in precipitation. The isotopic composition in TU-WS2 at the UP position also showed isotopic enrichment during the more isotopically depleted precipitation period during the first rainy season (Fig. 5h). Soil water at lower depths (SC2, WS2, and SC3) generally had more attenuated signals compared to precipitation and soil water at shallower soil layers (Fig. 5e-j) and showed less variation with topographic position.

The time series of the isotopic composition of water from wetlands and streamflow are presented in Fig. 6. Although the mean isotopic composition of water samples collected from CU-WE and streamflow presented a difference of 0.7‰ $\delta^{18}O$ (Fig. 4b-c), both water types had strongly attenuated isotopic compositions with almost negligible variation throughout the study period (Fig. 6a, and Fig. 6c). Even though TU-WE presented an attenuated signal during dry periods, its isotopic signal decreased during wetter periods when the isotopic composition of precipitation decreased (Fig. 6b).

3.3 Mixing processes along the catchment

As a proxy for water mixing processes within the catchment, we used the ITTP metric (Fig. 7). Streamflow at the catchment outlet presented the lowest ITTP value (0.01) amongst all sampling sites. The wetlands had ITTP values of 0.03 and 0.19 for the CU and TU wetlands, respectively. The soils´ ITTPs ranged between 0.04 and 0.49, and generally decreased with depth regardless of topographic position (Fig. 7). The shallower collectors SC1 and WS1 showed the highest ITTPs values and the largest range in ITTPs values for both the CU and TU hillslopes. At deeper soil collectors (SC2, WS2, SC3) the ITTP values were systematically low with values usually lower than 0.15. Although they showed some variation with depth, no clear differences were observed between sites or topographic positions.

Within the CU experimental hillslope, the UP-WS1 and LO-WS1 shallow collectors had ITTPs of 0.13 and 0.11, respectively. These values are smaller than ITTPs found in deeper soil layers such as UR-SC3 (0.14). The UP-SC3 showed the lowest ITTP of all along this experimental hillslope (0.08). Regarding the TU experimental hillslope, three shallow soil water sampling sites showed ITTPs lower than 0.16 (UP-SC1, LO-SC1, and MI-WS1). Similar to the CU hillslope, the ITTPs were small at sampling depths below SC2, generally lower than 0.20. Nevertheless, upper position sampling sites had the lowest ITTP, namely, UP-SC3 (0.04) and UP-SC2 (0.06).

4. DISCUSSION

4.1 Precipitation formation processes

The similar slope of the LMWL (8.2) and GMWL (8.0; Dansgaard, 1964; Rozanski et al., 1993) indicates that condensation prior to precipitation occurred under isotopic equilibrium conditions in the study area (Clark & Fritz, 1997; Kendall & McDonnell, 1998). This is likely related to the meteorological conditions of the high tropical Andes with low precipitation and temperature seasonality throughout the year (Célleri et al., 2007). The higher value of the intercept of the LMWL (16.2) compared to the GMWL (10) suggests that precipitation in the study area is likely influenced primarily by the isotopic composition of precipitation sourced from the Amazon basin. The latter is concluded based on the similar intercept of the LMWLs for high-elevation sites in the southern Andes of Ecuador (16.9-18.5), which has been attributed to the main influence of air moisture recycling from the Amazon forest on local precipitation with little influence of Pacific Ocean moisture (Esquivel-Hernández et al., 2019; Zhiña et al., 2022). Similar observations were made earlier by Gat & Matsui (1991), Salati et al. (1979), Garcia et al. (1998), in regional studies of stable isotope contents along two latitudinal transects across the Ecuadorian Andes where they reported intense recycling of water vapor in the Amazon Forest. The temporal dynamics of the isotopic composition of precipitation during the study period showed the so-called seasonal and amount effects (Rozanski et al., 1993). In effect, the isotopic composition of precipitation was enriched during the dryer periods when the precipitation input was low, whereas it was depleted during the rainy periods when precipitation input was high. Our results are in line with those reported at montane sites in the south Ecuadorian Andes (Mosquera et al., 2012; Windhorst et al., 2013) in which the slopes and intercepts of the LMWLs were close to 8 and larger than 10. Longer and finer temporal resolution precipitation isotopic records are necessary to carry out a thorough assessment of the origin of the air masses forming local precipitation and the factors influencing its isotopic composition.

4.2 Subsurface flow paths of water

The lc-excess values in soil water in the CU experimental hillslope were smaller than those in the TU experimental hillslope (Fig. 4), indicating that the isotopic composition of δ^2H changed at a faster rate than $\delta^{18}O$ in the soils of the former in comparison to those in the latter (Landwehr & Coplen, 2004; Leibundgut et al., 2009). From a hydrological point of view, these observations might indicate that soils under cushion forming plants are more prone to be affected by evaporation than those under tussock grasses since the latter presented lc-excess values closer to zero (i.e., similar to $\delta^{18}O$ in precipitation, Fig. 4). This difference could be related to plant phenology where tussock grasses with their long needles produce a shadow effect limiting evaporation from topsoil horizons, and where cushion forming plants (p.e., *Azorella pedunculata*) directly expose the topsoil to solar radiation. It is important to note that lc-excess values in soil water did not systematically decrease with depth (Fig. 4), which is also consistent with slight soil water evaporation from the topsoil.

Even though fog occurs periodically in the study area, it does not seem likely that it significantly increases soil moisture since around 96% of all the soil water samples had lc-excess values lower than zero, suggesting that rainfall is the major water source recharging soil moisture. This is in line with recent work by Berrones et al. (2022) who stated that fog is not a major contribution to the soil water budget due to the low height of the dominant páramo vegetation (tussock grass) in relation to the height at which fog occurs. However, further work is needed with fog or horizontal precipitation isotopic sampling to better assess the influence of these types of water inputs to soil moisture.

Streamflow and water sampled in wetlands also presented negative lc-excess values (Fig. 4), indicating that their isotopic signals were slightly affected by evaporation. Overall, the minor deviation of the isotopic composition of surface (i.e., streamflow) and subsurface (i.e., soil water and wetlands) samples from the LMWL (Fig. 3) indicates that the effect of fractionation by evaporation is small as has been reported for other high Andean sites in southern Ecuador (e.g., Mosquera et al., 2020a; Mosquera et al., 2016a). This can be the result of high infiltration rates and saturated hydraulic conductivity of volcanic ash topsoils (Mosquera et al., 2021; Páez-Bimos et al., 2022a).

In general, soil water isotopic signals were strongly attenuated with respect to the signal of precipitation, with only a few shallow soil layers resembling the temporal dynamic of the latter (Fig. 5). These observations imply that water stored in the soils is mainly composed of precipitation recharging the system before the sampling collection period (several months to few years ago; Mosquera et al., 2020a). Although the isotopic signals were roughly similar at most soil sampling sites, the diverse degree of soil water isotopic attenuation, especially at shallow sampling depths, depicts the complexity of water flow paths. For instance, an unexpected isotopic signal was observed in the TU-UP-WS2 (Fig. 5h), whose isotopic composition increased when the isotopic composition of rainfall decreased. Since this effect was not observed at other similar sampling positions or depths, it could be due to local pedological conditions above this sampler. These observations suggest that subsurface flow dynamics can vary at small spatial scales in line with zonal gradients in plant diversity and micro-topography (Molina et al., 2019; Paez-Bimos et al., 2022b; Sklenár & Ramsay, 2001). This was also found in other ecosystems (Kim & Jung, 2014; Kirchner, 2016; McDonnell et al., 1991).

Another seemingly unexpected effect was observed at the shallower samplers (SC1) in the TU hillslope (Fig. 5b). Apart from the UR position, all TU-SC1 samplers (installed at 15-25 cm depth) showed a smaller isotopic temporal variability than the TU-WS1 samplers (installed at 20-30 cm depth). The difference in isotopic signals between the two shallow collectors in the TU hillslope is most likely related to the type of sampler used (Orlowski et al., 2016; Sprenger et al., 2015, 2016). SCs collect water that is sucked out at a matric potential of 45-50 kPa, while WSs extract water at a much lower matric potential (5.4 kPa). This implies that soil water sampled using the SCs includes a fraction of mobile water molecules more attached to the soil matrix (i.e., at higher matric potential), which have remained in the soil system for longer periods (Paez-Bimos et al., 2022a). As a result, water from the SCs presented a stronger attenuation of the stable isotopic signal of soil water in comparison to the more mobile water sampled by the WSs located below. To test this hypothesis, isotopic data should be complemented with soil hydrophysical and geochemical information and soil moisture records in future investigations like in Sprenger et al. (2015).

The wetlands located below the CU and TU experimental hillslopes presented different temporal isotopic signals, particularly during the most humid periods (Fig. 6). Our data indicate that the isotopic response of the wetlands during rainy periods may be controlled by the geomorphological and topographical conditions of the sites where they were installed. The TU sampling site is situated in a topographic depression and located at the transition of the TU hillslope and the wetland (Paez-Bimos et al., 2022a). During rainy periods, part of the shallow soil horizons become hydrologically active and feed the wetland during storm events via subsurface lateral flow (Eguchi & Hasegawa, 2008; Hasegawa & Sakayori, 2000; McGuire & McDonnell, 2010; Mosquera et al., 2016a). During the less rainy periods, it appears that there is no hydrological connection between the shallow soil horizons of the TU hillslope and the TU wetland (Fig. 6b). In contrast, the strongly attenuated isotopic signal in CU presenting almost negligible variation throughout the whole study period (Fig. 6a.) probably results from its location: the CU wetland site is located at the center of a topographic depression (Fig. 1c), and the stagnation of water in the wetland leads to dampening of the isotopic signal. Similar findings have been reported for Andean wetlands in southern Ecuador (Lazo et al., 2019).

The strong attenuation of the isotopic signal that was observed in streamflow could be a result of the long water transit times in the hillslopes and/or the buffering capacity of the wetlands such as reported by Asano et al. (2002). However, the sole use of water stable isotopes does not allow to discriminate the dominant water sources in the catchment. Since the isotopic composition of streamflow did not resemble the temporal variability of precipitation, it can be expected that stream water age is longer than 5 years, i.e., the maximum age of water that can be estimated using the stable isotopes of water (Kendall & McDonnell, 1998; Leibundgut et al., 2009). Future research is needed in headwater basins underlain by Holocene volcanic deposits to determine water sources, estimate the age of water in different hydrological compartments, and quantify water storage capacity. Our data indicate that streamflow generation in tropical Andean catchments with thick volcanic ash soils and permeable bedrock differs from that in other Andean catchments with thin soils developed on hard bedrock with very low permeability (e.g., Lazo et al., 2019, Molina et al., 2019).

4.3 Water mixing in the catchment

Soil water at shallow depths (< 40 cm) slightly resembled the isotopic composition of precipitation (Fig. 5a-5d), suggesting a small influence of precipitation in mixing with water stored in soils (Mosquera et al., 2020a). At greater depths, the soil water isotopic composition showed strong damping and little variation with depth regardless of the sampling position. These effects are likely explained by the low hydraulic conductivity and high water retention capacity of deeper soil horizons (Páez-Bimos et al., 2022a). Similar ITTPs of soil water in deeper soil horizons (below 40 cm depth; Fig. 7) suggest preferential mixing of relatively old water (several months to few years old) in the system regardless of sampling depth. The soil water isotopic dynamics likely result from the combination of vertical and lateral water movement. Since the ITTPs do not show major variation with sampling position, and the experimental hillslopes have gentle slope gradients (≤20%), it is likely that vertical flow paths are important, particularly in the upper topographic positions (Fig. 8). The importance of vertical flow paths was also highlighted by Asano et al. (2002), Mosquera et al. (2020a), and Muñoz-Villers & McDonnell (2012) for other sites, even in steeper hillslopes where lateral flow paths could have been favored.

ITTPs have shown to be a good proxy of MTT values in several studies (e.g., Capell et al., 2012; Correa et al., 2017; Seeger & Weiler, 2014; Tetzlaff et al., 2009). It is worth noting that the isotopic attenuation observed in the study area is larger than in volcanic Andean catchments with shallow soils. In the Jatunhuaycu site, the collectors at 15-30 cm depth had ITTPs generally lower than 0.3 (Fig. 7), associated to MTTs larger than 6 months according to Tetzlaff et al. (2009). These MTTs values are longer than the MTT of approximately 1 month reported for soil water sampled at the same depth in an Andean catchment with shallow volcanic soils (<1 m) and bedrock with very low permeability (Correa et al., 2017; Lazo et al., 2019; Mosquera et al., 2020a). A similar pattern was observed for the MTTs at 40-60 cm depth, which presented ITTPs lower than 0.1 in our study site (Fig. 7; i.e., MTTs longer than 1 year following Tetzlaff et al. 2009), whereas MTTs of 3-5 months were reported for water sampled at the same depth in shallow volcanic soils in a southern Ecuador páramo site (Lazo et al., 2019; Mosquera et al., 2020a).

In another tropical volcanic environment, Muñoz-Villers & McDonnell (2012) reported shorter soil MTTs values in a montane cloud forest than those found in our study. Those authors found in the upper part of a hillslope (where no lateral flow would be expected) transit times of 20, 65, 91, and 139 days for depths of 30, 60, 90, and 120 cm, respectively. Here we found MTTs of 60-240 days for the 15-30 cm depths, and around 300-370 days for 40-60 cm depths according to the equivalence of ITTPs and MTTs presented by Tetzlaff et al. (2009). This is particularly interesting since those authors also reported a highly fractured underlying bedrock, which has shown to increase the MTT of volcanic sites in Japan and the Pacific Northwest in the United States (Asano & Uchida, 2012; Hale & McDonnell, 2016). To further understand the spatial variability and the lower ITTPs (larger MTT) values compared to other volcanic sites, a thorough understanding of the mechanisms controlling vertical and lateral water flow in the soil is needed.

Even though wetlands in páramos underlain by bedrock of very low permeability and shallow volcanic soils do not present isotopic signals as damped as in our study area (Lazo et al., 2019), it has been reported that they play a major role in catchment water storage (Roa-García & Weiler, 2010). The larger isotopic attenuation of wetlands and streamflow at our study site in comparison to sites with shallow soils shows that the buffering capacity of the wetlands in the study area is larger. Based on the difference in the average isotopic composition of wetlands and streamflow (0.7‰ $\delta^{18}O$), it seems that the temporal variability of their isotopic composition is almost negligible (except for the TU wetland during the driest periods, Fig. 6b), and that they are recharged by different sources (e.g., soil horizons at different depths, shallow versus deep water contributions) and/or during different time periods (e.g., precipitation recharging subsurface water reservoirs several months to years before the monitoring period) (Correa et al., 2018; Inamdar et al., 2013; Kirchner, 2003). The so-called altitudinal effect is not likely to cause this difference in isotopic composition since the difference in elevation between the upper and lower parts of the TU hillslope is only 65 m, and the $\delta^{18}O$ isotopic lapse rates in montane regions of the tropical Andes are around -0.3‰ per 100 m elevation increase (Mosquera et al., 2016a). Another potential factor causing such discrepancy could be the spatial distribution of rainfall with different isotopic composition. However, given the small areal extent of our site (0.68 km^2) this factor is not likely to explain the observed differences either. Long-term rainfall monitoring using a gradient-based, spatially distributed network of rainfall samplers is necessary to further investigate this issue.

Our results indicate that the hydrological behavior of Andean páramo catchments influenced by Holocene volcanism is characterized by subsurface flow paths in the soil mantle and underlying parent material that possess water ages longer than 5 years. Although this reservoir could not be clearly defined, the strong attenuation of the isotopic signals of surface and subsurface waters suggests that it may be composed of water from deeper soil horizons and/or groundwater contributions favored by the permeable geology (Fig. 8). This reservoir may mix with water stored in the wetlands, pointing to the key role deep subsurface flow through deep and buried horizons of volcanic soils play in the hydrological behavior of the system, even during stormflow events (Silva Palmay & Ortiz Moya, 2020). These findings contrast with the subsurface hydrological behavior of catchments in the tropical Andes that present thin soils developed on volcanic bedrock with very low permeability, where the hydrology is controlled by shallow subsurface flow through the organic horizon (30-40 cm depth) of the soil (Mosquera et al., 2016a).

5. CONCLUSIONS

This study focused on the hydrology of a headwater Andean catchment influenced by Holocene volcanic activity, and is based on the analysis of the stable isotopes of water. To this end, biweekly data of the isotopic composition of precipitation, soil water, wetlands, and streamflow were analyzed. Precipitation at the study site seems to occur under equilibrium conditions, whereby local precipitation might be influenced by recycled moisture from the Amazon Basin. Water sampled from soils, wetlands, and streamflow are little affected by evaporation effects, although future investigation should assess this effect in the topsoil where the evaporation effect could be important. The isotopic attenuation of soil water generally increased with depth regardless of topographic position and vegetation cover (i.e., tussock grass and cushion plant), except for the shallowest samplers in the tussock grass slope. Water from wetlands and river showed an almost invariant isotopic composition as compared to precipitation during the study period, which might be indicative of waters older than 5 years contributing to streamflow via deep subsurface flow through deep and buried volcanic soil horizons, ash layers, and fractured bedrock. Although ITTPs showed a decreasing trend with depth, there exist local variation that might be related to hydrophysical soil properties. The low hydraulic conductivity and high water retention capacity of the volcanic soils in combination with relatively small annual water inputs compared to humid areas in the tropical Andes likely explain the strong isotopic attenuation of water in deeper soil horizons, wetlands, and streamflow. These observations show the importance of understanding the local pedological and geological context in regions influenced by recent volcanism for soil water monitoring and modelling. In addition, the obtained knowledge can help to develop strategies for sustainable water resources management to secure water availability to supply human needs. Future research work could therefore include identifying the main water sources contributing to streamflow during variable flow conditions (from baseflow to rainstorm events), determining the age of surface and subsurface waters, estimating catchment water storage, and assessing the effect of different land restoration practices on catchment hydrology. Finally, the isotopic information can also be used in combination with geochemical, hydrophysical, and high frequency tracer data to further improve the process-based understanding of the hydrology of Andean catchments influenced by recent or active volcanism.

ACKNOWLEDGEMENTS

We thank FONAG and EPMAPS-Q for facilitating the experimental work within the Jatunhuaycu catchment. The ParamoSus project and its team carried out the characterization of soils, installed the field equipment, and conducted the biweekly sampling of water in soils, wetlands, and streamflow. The members of the team are: B. De Bièvre, M. Calispa, P. Delmelle, A. Molina, T. Munoz, R. Osorio, S. Páez-Bimos, V. Vanacker, and M. Villacis (in alphabetical order). Isaías Quinatoa and Jordan Cruz, undergraduate students of the Department of Civil and Environmental Engineering of the E.P.N, are thanked for their field and lab assistance. This manuscript is an outcome of the Hydrology Master Program at the University of Cuenca.

FUNDING

This research was funded by the ARES, l'Académie de Recherche et d'Enseignement supérieur de la Fédération Wallonie-Bruxelles (Belgium) through the project "ParamoSUS: Linking Global Change with Soil and Water Conservation in the High Andes". G.M.M. is supported by a Postdoctoral Fellowship from the Universidad San Francisco de Quito and the H2020 European Research and Innovation action Grant Agreement N°869226 (DRYvER).

AUTHOR CONTRIBUTIONS

Conceptualization, GMM; Methodology, BL, GMM, PC, VV, XZR; Experimental Design: VV, SPB, MC; Data collection: SPB, MC; Data analysis, BL, GMM; Literature Review, BL; GMM, VV, SPB; Funding acquisition, VV; Project administration, VV; Supervision, GMM; Writing—original draft, BL, GMM; Writing—review and editing, all authors. All authors have read and agreed to the published version of the manuscript.

DATA AVAILABILITY STATEMENT

The data that support the findings of this study are available from the corresponding author upon reasonable request.

6. References

Aparecido, L. M. T., Teodoro, G. S., Mosquera, G., Brum, M., de V. Barros, F., Pompeu, P. V., Rodas, M., Lazo, P., Müller, C. S., Mulligan, M., Asbjornsen, H., Moore, G. W., & Oliveira, R. S. (2017). Ecohydrological drivers of Neotropical vegetation in montane ecosystems. *Ecohydrology*, *11*(3). https://doi.org/10.1002/eco.1932

Asano, Y., Uchida, T., & Ohte, N. (2002). Residence times and flow paths of water in steep unchannelled catchments, Tanakami, Japan. *Journal of Hydrology*, *261*(1–4), 173–192. https://doi.org/10.1016/S0022-1694(02)00005-7

Asano, Y., & Uchida, T. (2012). Flow path depth is the main controller of mean base flow transit times in a mountainous catchment. Water Resources Research, 48(3), 1–8. https://doi.org/10.1029/2011WR010906

Brooks, J. R., Wigington, P. J., Phillips, D. L., Comeleo, R., & Coulombe, R. (2012). Willamette River Basin surface water isoscape (δ 18 O and δ 2 H): temporal changes of source water within the river. *Ecosphere*, *3*(5), art39. https://doi.org/10.1890/es11-00338.1

Buytaert, W., & Bièvre, B. De. (2012). Water for cities: The impact of climate change and demographic growth in the tropical Andes. *Water Resources Research*, *48*(8), 1–13. https://doi.org/10.1029/2011WR011755

Buytaert, W., Wyseure, G., Bièvre, B. De, & Deckers, J. (2005). The effect of land-use changes on the hydrological behaviour of Histic Andosols in south Ecuador. *Hydrological Processes*, *19*(20), 3985–3997. https://doi.org/10.1002/hyp.5867

Buytaert, W., Deckers, J., & Wyseure, G. (2007). Regional variability of volcanic ash soils in south Ecuador: The relation with parent material, climate and land use. CATENA, 70(2), 143–154. https://doi.org/10.1016/J.CATENA.2006.08.003

Calispa, M., Ypersele, R. van, Pereira, B., Páez-Bimos, S., Vanacker, V., Villacís, M., Molina, A., Bièvre, B. de, Muñoz, T., & Delmelle, P. (2021). Soil organic carbon stocks under different páramo vegetation covers in Ecuador's northern Andes. *EGU General Assembly 2021*. https://doi.org/10.5194/EGUSPHERE-EGU21-4121

Capell, R., Tetzlaff, D., Hartley, A. J., & Soulsby, C. (2012). Linking metrics of hydrological function and transit times to landscape controls in a heterogeneous mesoscale catchment. Hydrological Processes, 26(3), 405–420. https://doi.org/10.1002/hyp.8139

Célleri, R., & Feyen, J. (2009). The Hydrology of Tropical Andean Ecosystems: Importance, Knowledge Status, and Perspectives. *Mountain Research and Development*, *29*(4), 350–355. https://doi.org/10.1659/mrd.00007

Célleri, R., Willems, P., Buytaert, W., & Feyen, J. (2007). Space–time rainfall variability in the Paute Basin, Ecuadorian. *HYDROLOGICAL PROCESSES*, *24*(1), 318–326. https://doi.org/10.1002/hyp.6575

Clark, I., & Fritz, P. (1997). Environmental Isotopes in Hydrogeology. In *Water Encyclopedia*. https://doi.org/10.1002/047147844X.gw211

Correa, A., Breuer, L., Crespo, P., Célleri, R., Feyen, J., Birkel, C., Silva, C., & Windhorst, D. (2018). Spatially distributed hydro-chemical data with temporally high-resolution is needed to adequately assess the hydrological functioning of headwater catchments. *Science of The Total Environment*, *651*, 1613–1626. https://doi.org/10.1016/j.scitotenv.2018.09.189

Correa, A., Windhorst, D., Tetzlaff, D., Crespo, P., Célleri, R., Feyen, J., & Breuer, L. (2017). Temporal dynamics in dominant runoff sources and flow paths in the Andean Páramo. *Water Resources Research*, *53*(7), 5998–6017. https://doi.org/10.1002/2016WR020187

Craig, H. (1961). Standard for Reporting Concentrations of Deuterium and Oxygen-18 in Natural Waters. *Science*, *133*(1958), 18–19.

Crespo, P. J., Feyen, J., Buytaert, W., Bücker, A., Breuer, L., Frede, H. G., & Ramírez, M. (2011). Identifying controls of the rainfall-runoff response of small catchments in the tropical Andes (Ecuador). *Journal of Hydrology*, *407*(1–4), 164–174. https://doi.org/10.1016/j.jhydrol.2011.07.021

Dansgaard, W. (1964). Stable isotopes in precipitation. *Tellus*, *16*(4), 436–468. https://doi.org/10.3402/tellusa.v16i4.8993

Eguchi, S., & Hasegawa, S. (2008). Determination and Characterization of Preferential Water Flow in Unsaturated Subsoil of Andisol. *Soil Science Society of America Journal*, *72*(2), 320–330. https://doi.org/10.2136/sssaj2007.0042

EPMAPS, & FONAG. (2018). *Actualización del plan de manejo del área de conservación hídrica Antisana*. 99.

Erauw, A. (2019). Soil horizon thickness as indicator of soil production and transport along slopes. MSc Thesis, Faculty of Sciences, Université catholique de Louvain.

Esquivel-Hernández, G., Mosquera, G. M., Sánchez-Murillo, R., Quesada-Román, A., Birkel, C., Creespo, P., Célleri, R., Windhorst, D., Breuer, L., & Boll, J. (2019). Moisture transport and seasonal variations in the stable isotopic composition of rainfall in Central American and Andean Páramo during El Niño conditions (2015-2016). *Hydrological Processes*. https://doi.org/10.1002/hyp.13438

FAO. (2015). *World reference base for soil resources 2014 International soil classification system*.

Garcia, M., Villalba, F., Araguás-Araguás, L., & Rozanski, K. (1998). The role of atmospheric circulation patterns in controlling the regional distribution of stable isotope contents in precipitation: Preliminary results from two transects in the Ecuadorian Andes. International Atomic Energy Agency (IAEA): IAEA.

Gat, J. R., & Matsui, E. (1991). Atmospheric water balance in the Amazon basin: An isotopic evapotranspiration model. *Journal of Geophysical Research*, *96*(D7), 13179. https://doi.org/10.1029/91JD00054

Gébelin, A., Witt, C., Radkiewicz, M., & Mulch, A. (2021). Impact of the Southern Ecuadorian Andes on Oxygen and Hydrogen Isotopes in Precipitation. Frontiers in Earth Science, 9(May), 1–9. https://doi.org/10.3389/feart.2021.664590

Grubb, P. J., Lloyd, J. R., Pennington, T. D., & Páez-Bimos, S. (2020). A historical baseline study of the páramo of Antisana in the Ecuadorian Andes including the impacts of burning, grazing and trampling. 13(3–4), 225–256. https://doi.org/10.1080/17550874.2020.1819464

Hale, V. C., & McDonnell, J. J. (2016). Effect of bedrock permeability on stream base flow mean transit time scaling relations: 1. A multiscale catchment intercomparison. Water Resources Research, 52(2), 1358–1374. https://doi.org/https://doi.org/10.1002/2014WR016124

Hall, M. L., Mothes, P. A., Samaniego, P., Militzer, A., Beate, B., Ramón, P., & Robin, C. (2017). Antisana volcano: A representative andesitic volcano of the eastern cordillera of Ecuador: Petrography, chemistry, tephra and glacial stratigraphy. *Journal of South American Earth Sciences*, *73*, 50–64. https://doi.org/10.1016/j.jsames.2016.11.005

Hasegawa, S., & Sakayori, T. (2000). Monitoring of matrix flow and bypass flow through the subsoil in a volcanic ash soil. *Soil Science and Plant Nutrition*, *46*(3), 661–671. https://doi.org/10.1080/00380768.2000.10409131

Hrachowitz, M., Benettin, P., van Breukelen, B. M., Fovet, O., Howden, N. J. K., Ruiz, L., van der Velde, Y., & Wade, A. J. (2016). Transit times-the link between hydrology and water quality at the catchment scale. *Wiley Interdisciplinary Reviews: Water*, *3*(5), 629–657. https://doi.org/10.1002/wat2.1155

Inamdar, S., Dhillon, G., Singh, S., Dutta, S., Levia, D., Scott, D., Mitchell, M., Stan, J. Van, & McHale, P. (2013). Temporal variation in end-member chemistry and its influence on runoff mixing patterns in a forested, Piedmont catchment. *Water Resources Research*, *49*(4), 1828–1844. https://doi.org/10.1002/wrcr.20158

Kendall, C., & Coplen, T. B. (2001). *Distribution of oxygen-18 and deuterium in river waters across the United States*. *1393*(September 2000), 1363–1393. https://doi.org/10.1002/hyp.217

Kendall, C., & McDonnell, J. J. (1998). *Isotope Tracers in Catchment Hydrology*. *80*(23), 1999. https://doi.org/10.1016/C2009-0-10239-8

Kim, S., & Jung, S. (2014). Estimation of mean water transit time on a steep hillslope in South Korea using soil moisture measurements and deuterium excess. *Hydrological Processes*, *28*(4), 1844–1857. https://doi.org/10.1002/hyp.9722

Kirchner, J. W. (2003). A double paradox in catchment hydrology and geochemistry. *Hydrological Processes*, *17*(4), 871–874. https://doi.org/10.1002/hyp.5108

Kirchner, J. W. (2016). Aggregation in environmental systems-Part 1: Seasonal tracer cycles quantify young water fractions, but not mean transit times, in spatially heterogeneous catchments. *Hydrology and Earth System Sciences*, *20*(1), 279–297. https://doi.org/10.5194/hess-20-279-2016

Landwehr, J. M., & Coplen, T. B. (2004). Line-conditioned excess: A new method for characterizing stable hydrogen and oxygen isotope ratios in hydrologic systems. http://inis.iaea.org/search/search.aspx?orig_q=RN:36008379

Lazo, P. X., Mosquera, G. M., McDonnell, J. J., & Crespo, P. (2019). The role of vegetation, soils, and precipitation on water storage and hydrological services in Andean Páramo catchments. *Journal of Hydrology*, *572*, 805–819. https://doi.org/10.1016/j.jhydrol.2019.03.050

Leibundgut, C., Maloszewski, P., & Külls, C. (2009). *Tracers in Hydrology* (H. Leistert & I. Kohn (eds.)). Wiley-Blackwell. ISBN: 978-0-470-51885-4

McDonnell, J. J., Owens, I. F., & Stewart, M. K. (1991). a Case Study of Shallow Flow Paths IN A STEEP ZERO-ORDER BASIN. *Water Resources Bulletin*, *27*(4), 679–685. https://doi.org/10.1111/j.1752-1688.1991.tb01469.x

McGuire, K. J., & McDonnell, J. J. (2006). A review and evaluation of catchment transit time modeling. *Journal of Hydrology*, *330*(3–4), 543–563. https://doi.org/10.1016/j.jhydrol.2006.04.020

McGuire, K. J., & McDonnell, J. J. (2010). Hydrological connectivity of hillslopes and streams: Characteristic time scales and nonlinearities. *Water Resources Research*, *46*(10), 1–17. https://doi.org/10.1029/2010WR009341

Minaya, V., Camacho Suarez, V., Wenninger, J., & Mynett, A. (2016). Quantification of runoff generation from a combined glacier and páramo catchment within an Ecological Reserve in the Ecuadorian highlands. *Hydrology and Earth System Sciences Discussions*, *November*, 1–20. https://doi.org/10.5194/hess-2016-569

Molina, A., Vanacker, V., Corre, M. D., & Veldkamp, E. (2019). Patterns in Soil Chemical Weathering Related to Topographic Gradients and Vegetation Structure in a High Andean Tropical Ecosystem. *Journal of Geophysical Research: Earth Surface*, *124*(2), 666–685. https://doi.org/10.1029/2018JF004856

Mook, W. G. (2000). Environmental isotopes in the hydrological cycle, principles and applications. Volume III: Surface water. *International Atomic Energy Agency*, *1*(39), 1–291. http://www.hydrology.nl/images/docs/ihp/Mook_VI.pdf

Moore, R. D. (2005). Introduction to Salt Dilution Gauging for Streamflow Measurement Part III : Slug Injection Using Salt in Solution.

Mosquera, G. M., Lazo, P., Cárdenas, I., & Crespo, P. (2012). Identificación de las principales fuentes de agua que aportan a la generación de escorrentía en zonas Andinas de páramo húmedo: mediante el uso de los isótopos estables deuterio y oxígeno-18. *MASKANA*, *3*(2), 87–105. https://doi.org/10.18537/mskn.03.02.07

Mosquera, G. M., Lazo, P., Célleri, R., Wilcox, B., & Crespo, P. (2015). Runoff from tropical alpine grasslands increases with areal extent of wetlands. Catena, 125, 120–128. https://doi.org/10.1016/j.catena.2014.10.010

Mosquera, G. M., Célleri, R., Lazo, P. X., Vaché, K. B., Perakis, S. S., & Crespo, P. (2016a). Combined use of isotopic and hydrometric data to conceptualize ecohydrological processes in a high-elevation tropical ecosystem. *Hydrological Processes*, *30*(17), 2930–2947. https://doi.org/10.1002/hyp.10927

Mosquera, G. M., Segura, C., Vaché, K. B., Windhorst, D., Breuer, L., & Crespo, P. (2016b). Insights into the water mean transit time in a high-elevation tropical ecosystem. *Hydrology and Earth System Sciences*, *20*(7), 2987–3004. https://doi.org/10.5194/hess-20-2987-2016

Mosquera, G. M., Crespo, P., Breuer, L., Feyen, J., & Windhorst, D. (2020a). Water transport and tracer mixing in volcanic ash soils at a tropical hillslope: A wet layered sloping sponge. *Hydrological Processes*, *34*(9), 2032–2047. https://doi.org/10.1002/hyp.13733

Mosquera, G. M., Marín, F., Jan, F., Rolando, C., Lutz, B., David, W., & Patricio, C. (2020b). A field, laboratory, and literature review evaluation of the water retention curve of volcanic ash soils: How well do standard laboratory methods reflect field conditions? *Hydrological Processes*, 35(1), 1–18. https://doi.org/10.1002/hyp.14011

Mosquera G.M., Marín F, Stern M, Bonnesoeur V, Ochoa-Tocachi BF, Román-Dañobeytia F, Crespo

P. (2021). Progress in understanding the hydrology of high-elevation Andean grasslands under changing land use. *Science of the Total Environment* 804: 150112. https://doi.org/10.1016/j.scitotenv.2021.150112

Muñoz-Villers, L. E., Geissert, D. R., Holwerda, F., & McDonnell, J. J. (2016). Factors influencing stream baseflow transit times in tropical montane watersheds. *Hydrology and Earth System Sciences*, *20*(4), 1621–1635. https://doi.org/10.5194/hess-20-1621-2016

Muñoz-Villers, L. E., & McDonnell, J. J. (2012). Runoff generation in a steep, tropical montane cloud forest catchment on permeable volcanic substrate. *Water Resources Research*, *48*(9), 1–17. https://doi.org/10.1029/2011WR011316

Nierop, K. G. J., Tonneijck, F. H., Jansen, B., & Verstraten, J. M. (2007). Organic Matter in Volcanic Ash Soils under Forest and Páramo along an Ecuadorian Altitudinal Transect. Soil Science Society of America Journal, 71(4), 1119–1127. https://doi.org/10.2136/SSSAJ2006.0322

Ochoa-Tocachi, B. F., Buytaert, W., Bièvre, B. De, Célleri, R., Crespo, P., Villacís, M., Llerena, C. A., Acosta, L., Villazón, M., Guallpa, M., Gil-Ríos, J., Fuentes, P., Olaya, D., Viñas, P., Rojas, G., & Arias, S. (2016). Impacts of land use on the hydrological response of tropical Andean catchments. *Hydrological Processes*, *30*(22), 4074–4089. https://doi.org/10.1002/hyp.10980

Onderet, C. (2018). *Impact des changements de végétation sur les propriétés des sols des páramos équatoriens : étude de cas dans la réserve de l'Antisana*. Master thesis of Faculty of Bioengineering, Université Catholique de Louvain.

Orlowski, N., Pratt, D. L., & McDonnell, J. J. (2016). Intercomparison of soil pore water extraction methods for stable isotope analysis. Hydrological Processes, 30(19), 3434–3449. https://doi.org/https://doi.org/10.1002/hyp.10870

Oshun, J., Dietrich, W., Dawson, T., & Fung, I. (2015). Dynamic, structured heterogeneity of water isotopes inside hillslopes. *Water Resources Research*, *51*, 5974–5997. https://doi.org/10.1002/2014WR015608.Received

Páez-Bimos, S., Vanacker, V., Villacis, M., Calispa, M., Morales, O., Molina, A., Delmelle, P., Lahuatte, B., De Bievre, B., and Muñoz, T. (2021): Linking soil water and solutes fluxes to soil properties and vegetation types: insights from a case-study in the high tropical Andes of Ecuador, *EGU General Assembly 2021*, online, 19–30 Apr 2021, EGU21-7934. https://doi.org/10.5194/egusphere-egu21-7934

Páez-Bimos, S., Villacís, M., Morales, O., Calispa, M., Molina, A., Salgado, S., de Bievre, B., Delmelle, P., Muñoz, T., & Vanacker, V. (2022a). Vegetation effects on soil pore structure and hydraulic properties in volcanic ash soils of the high Andes. Hydrological Processes, n/a(n/a), e14678. https://doi.org/10.1002/hyp.14678

Páez-Bimos, S., Molina, A., Calispa, M., Delmelle, P., Lahuatte, B., Villacís, M., Muñoz, T., and Vanacker (2022b), V.: Soil-vegetation-water interactions controlling solute flow and transport in volcanic ash soils of the high Andes, Hydrol. Earth Syst. Sci. Discuss. [preprint], https://doi.org/10.5194/hess-2022-294, in review,.

Ramón J, Correa A, Timbe E, Mosquera GM, Mora E, Crespo P. (2021). Do mixing models with different input requirement yield similar streamflow source contributions? Case study: A tropical montane catchment. *Hydrological Processes* 35 (6): e14209. https://doi.org/10.1002/hyp.14209

Roa-García, M. C., & Weiler, M. (2010). Integrated response and transit time distributions of watersheds by combining hydrograph separation and long-term transit time modeling. Hydrology and Earth System Sciences, 14(8), 1537–1549. https://doi.org/10.5194/hess-14-1537-2010

Rozanski, K., Araguás-Araguás, L., & Gonfiantini, R. (1993). *Isotopic Patterns in Modern Global Precipitation*. 1–36. https://doi.org/10.1029/GM078p0001

Salati, E., Dall'Olio, A., Matsui, E., & Gat, J. R. (1979). Recycling of water in the Amazon Basin: An isotopic study. *Water Resources Research*, *15*(5), 1250–1258. https://doi.org/10.1029/WR015i005p01250

Seeger, S., & Weiler, M. (2014). Reevaluation of transit time distributions, mean transit times and their relation to catchment topography. Hydrology and Earth System Sciences, 18(12), 4751–4771. https://doi.org/10.5194/hess-18-4751-2014

Silva Palmay, L. F., & Ortiz Moya, E. W. (2020). *Caracterización isotópica de un evento de crecida sobre la microcuenca 1 del Río Jatunhuaycu*. http://www.dspace.uce.edu.ec/handle/25000/20654

Singh, G., Kaur, G., Williard, K., Schoonover, J., & Kang, J. (2018). Monitoring of Water and Solute Transport in the Vadose Zone: A Review. *Vadose Zone Journal*, *17*(1), 160058. https://doi.org/10.2136/vzj2016.07.0058

Sklenár, P., & Ramsay, P. M. (2001). Diversity of zonal páramo plant communities in Ecuador. *Diversity and Distributions*, 7(3), 113–124. https://doi.org/10.1046/J.1472-4642.2001.00101.X

Sprenger, M., Herbstritt, B., & Weiler, M. (2015). Established methods and new opportunities for pore water stable isotope analysis. Hydrological Processes, 29(25), 5174–5192. https://doi.org/https://doi.org/10.1002/hyp.10643

Sprenger, M., Leistert, H., Gimbel, K., & Weiler, M. (2016). Illuminating hydrological processes at the soil-vegetation-atmosphere interface with water stable isotopes. Reviews of Geophysics, 54(3), 674–704. https://doi.org/https://doi.org/10.1002/2015RG000515

Tenorio, G. E., Vanacker, V., Campforts, B., Álvarez, L., Zhiminaicela, S., Vercruysse, K., Molina, A., & Govers, G. (2018). Tracking spatial variation in river load from Andean highlands to inter-Andean valleys. Geomorphology, 308, 175–189. https://doi.org/10.1016/j.geomorph.2018.02.009

Tetzlaff, D., Seibert, J., McGuire, K. J., Laudon, H., Burns, D. A., Dunn, S. M., & Soulsby, C. (2009). How does landscape structure influence catchment transit time across different geomorphic provinces? *Hydrological Processes*, *23*(6), 945–953. https://doi.org/https://doi.org/10.1002/hyp.7240

Tonneijck, F. H., Hageman, J. A., Sevink, J., & Verstraten, J. M. (2008). Tephra stratification of volcanic ash soils in Northern Ecuador. Geoderma, 144(1–2), 231–247. https://doi.org/10.1016/J.GEODERMA.2007.11.009

Torres, S., & Proaño, C. (2018). Water balance components in the Paramo of Jatunsacha, Ecuador. Granja, 28(2), 52–66. https://doi.org/10.17163/lgr.n28.2018.04

Vanacker V, Molina A, Torres R, Calderon E, Cadilhac L. (2018). Challenges for research on global change in mainland Ecuador. Neotropical Biodiversity 4 (1): 114–118 https://doi.org/10.1080/23766808.2018.1491706

Vanacker, V., Molina, A., Rosas-Barturen, M., Bonnesoeur, V., Román-Dañobeytia, F., Ochoa-Tocachi, B. F., and Buytaert, W. (2022): The effect of natural infrastructure on water erosion mitigation in the Andes, SOIL, 8, 133–147, https://doi.org/10.5194/soil-8-133-2022

Walsh, R. P. D., & Lawler, D. M. (1981). RAINFALL SEASONALITY: DESCRIPTION, SPATIAL PATTERNS AND CHANGE THROUGH TIME. Weather, 36(7), 201–208. https://doi.org/https://doi.org/10.1002/j.1477-8696.1981.tb05400.x

Windhorst, D., Waltz, T., Timbe, E., Frede, H. G., & Breuer, L. (2013). Impact of elevation and weather patterns on the isotopic composition of precipitation in a tropical montane rainforest. *Hydrology and Earth System Sciences*, *17*(1), 409–419. https://doi.org/10.5194/hess-17-409-2013

Wright, C., Kagawa-Viviani, A., Gerlein-Safdi, C., Mosquera, G. M., Poca, M., Tseng, H., & Chun, K. P. (2017). Advancing ecohydrology in the changing tropics: Perspectives from early career scientists. *Ecohydrology*, *11*(3), 1–18. https://doi.org/10.1002/eco.1918

Zhiña, D. X., Mosquera, G. M., Esquivel-Hernández, G., Córdova, M., Sánchez-Murillo, R., Orellana-Alvear, J., & Crespo, P. (2022). Hydrometeorological factors controlling the stable isotopic composition of precipitation in the highlands of south Ecuador. Journal of Hydrometeorology, 23(4), 1059–1074. https://doi.org/10.1175/JHM-D-21-0180.1

Table 1. Characterization of the soil pits located within the tussock grass (TU) and cushion plant (CU) experimental hillslopes (Calispa et al., 2021). UP, UR, MI. and LO correspond to upper, upper replica, middle, and lower sampling positions along each of the experimental hillslopes, respectively.

Position	Altitude (m.a.s.l.)	Soil Horizon depth (cm)				
		O	A	2A	2BC	3BC
TU-UR	4227	0-5	5-40	40-70	70-85	85-120
TU-UP	4225	0-5	5-30	30-60	60-85	85-110
TU-MI	4185	0-5	4-27	27-70	70-95	95-115
TU-LO	4161	0-7	7-45	45-92	92-110	110-135
CU-UR	4196	0-8	8-30	30-55	55-80	80-102
CU-UP	4197	0-8	8-30	30-60	60-80	80-102
CU-MI	4184	0-8	8-32	32-70	70-103	103-125
CU-LO	4173	0-10	10-40	40-75	75-110	110-120

Table 2. Depth of installation of the soil water samplers (suction cups or SCs, and wick samplers or WS) along the tussock grass (TU) and cushion plants (CU) experimental hillslopes. UP, UR, MI. and LO correspond to upper, upper replica, middle, and lower sampling position, respectively.

Sampling position	Sampler depth (cm)				
	A[1]	A-2A[1]	2A[1]	2A-2BC[1]	2,3 BC [1]
	SC1[2]	WS1[2]	SC2[2]	WS2[2]	SC3[2]
TU-UR	15	25	45	50	87
TU-UP	25	20	51	55	102
TU-MI	15	30	55	60	110
TU-LO	20	30	60	70	100
CU-UR	20	30	40	50	80
CU-UP	20	30	50	60	90
CU-MI	23	25	50	60	92
CU-LO	23	35	53	58	90

Note:
[1] Refers to a soil layer or transition between two soil layers in which a soil water sampler was installed.
[2] SC and WS stand for suction cup and wick sampler, respectively.

List of Figures

Figure 1. a) Location of the Jatunhuaycu Experimental Observatory (JEO) in the northern Ecuadorian Andes. b) Subcatchment 1 (JTU_01; black area) within the JEO marked with a yellow line. c) Monitoring setup at JTU_01 including the Tussock grass (TU, red circles) and Cushion plant (CU, green circles) experimental hillslopes showing the location of the soil water samplers at the upper (UP), upper replica (UR), middle (MI), and lower (LO) parts of the hillslope, the wetlands (WE) at the bottom of each hillslope (blue circles), and streamflow station (white circle). Subplot c) also shows an example of a representative profile of the soils monitored at the TU and CU experimental hillslopes (horizons A, 2A, 2BC) within the catchment (Calispa et al., 2021). Suction cups (SC) were used to collect soil water at the middle of the A, 2A, and 2BC horizons and wick samplers (WS) were used to collect soil water at the interface of the A-2A and 2A-2BC horizons as indicated by the open circles in the profile. Water from wetlands was sampled using a well at the bottom of each experimental hillslope. A rain gauge and a self-made precipitation water sampler were installed at the upper part of the CU hillslope. For a better reference of the soils and samplers' depth we refer the reader to Tables 1 and 2. The dotted lines correspond to the transects used in the conceptual model presented in Figure 8 (Tussock grass transect, orange line; and Cushion plant transect, green line).

Figure 2. a) Biweekly time series of precipitation amount (grey bars) and $\delta^{18}O$ isotopic composition (blue line). b) $\delta^{18}O$-$\delta^{2}H$ relation in local precipitation showing the local meteoric water line (LMWL) and the global meteoric water line (GMWL). c) Hourly streamflow time series (blue line) showing the time of collection of streamflow water samples for stable isotope analysis (red dots). Streamflow data gaps are due to failure of the pressure sensor used to measure water level. The Vienna-Standard Mean Ocean Water (V-SMOW) was used as reference to report $\delta^{18}O$ isotopic values.

Figure 3. $\delta^{18}O$-$\delta^{2}H$ relation in soil water collected using suction cups (SC) and wick samplers (WS) at the upper (UP), upper replica (UR), middle (MI), and lower (LO) parts of the cushion plant (CP) and tussock grass (TU) experimental hillslopes, the wetlands (WE) at the bottom of each hillslope, and streamflow at the catchment outlet (Q). Samples were collected biweekly during the period March 2019-February 2020. Sampling depths for each soil water sampler are shown next to the sampler code. The Vienna-Standard Mean Ocean Water (V-SMOW) was used as reference to report $\delta^{18}O$ isotopic values.

Figure 4. Boxplots of $\delta^{18}O$ and lc-excess for soil water, wetlands, and streamflow samples. Data representation responds to the transects presented in Figure 1 and Figure 8. TU hillslope goes from left to right from upper to lower positions, and from shallower to deeper samplers. CU hillslope goes from right to left from upper to lower positions, and from shallower to deeper samplers. Center plot corresponds to streamflow where both hillslopes drained. The Vienna-Standard Mean Ocean Water (V-SMOW) was used as reference to report $\delta^{18}O$ isotopic values. Line-conditioned excess (lc-excess, Landwehr & Coplen, 2004) was calculated using the following equation: lc-excess = $\delta^{2}H - a*\delta^{18}O - b$, where a and b are the LMWL's slope and intercept, respectively.

Figure 5. Time series of the biweekly isotopic composition of precipitation (blue lines) and soil water collected using suction cups (SC) and wick samplers (WS) at the upper (UP), upper replica (UR), middle (MI), and lower (LO) parts of the cushion plant (CP) and tussock grass (TU) experimental hillslopes during the period March 2019-February 2020. Sampling depth for each soil water sampler is shown in Table 2. The Vienna-Standard Mean Ocean Water (V-SMOW) was used as reference to report $\delta^{18}O$ isotopic values.

Figure 6. Time series of the biweekly isotopic composition of precipitation (blue lines), wetlands (WE) at the bottom of the cushion plant (CU) and tussock grass (TU) experimental hillslopes, and

streamflow at the catchment outlet (Q) during the period March 2019-February 2020. The Vienna-Standard Mean Ocean Water (V-SMOW) was used as reference to report $\delta^{18}O$ isotopic values.

Figure 7. Inverse Transit Time Proxies (ITTPs) of soil water collected using suction cups (SC) and wick samplers (WS) at the upper (UP), upper replica (UR), middle (MI), and lower (LO) parts of the cushion plant (CU) and tussock grass (TU) experimental hillslopes versus sampling depth. Sampling depths for each soil water sampler are shown in Table 2. The green dashed and black solid vertical lines show the ITTPs of wetlands (WE) at each experimental hillslope and streamflow (Q) at the outlet of the catchment, respectively.

Figure 8. Delineation of water flow paths in a tropical Andean headwater catchment shaped by recent (Holocene) volcanic activity within the Jatunhuaycu Experimental Observatory. Suction cups (SC) and wick samplers (WS) were installed for soil water monitoring and two wells were implemented for water sampling in wetlands (WE) along the hillslopes covered by tussock grass and cushion plants. The arrows represent the relative importance of various water flow paths as depicted by the stable isotopic composition and inverse transit time proxies (ITTPs shown as blue circles) of soil water at the upper (UP), upper replica (UR), middle (MI), and lower (LO) parts of the hillslope, wetlands (WE), and stream water (Q). The green arrows show the dominance of vertical flow in the volcanic soil layers in the hillslope positions. The yellow arrows refer to deeper subsurface flows being the main contributors of water to streamflow, and include water flow in buried soil horizons and ash layers, wetlands, and fractures on permeable parent material. The small red arrows point to the fact that surface water flow is negligible in the study catchment. Note: For illustrative purposes, the thickness of the upper soil horizons is not to scale and remains constant along slopes. We refer the reader to Tables 1 and 2 for the exact thickness of the soil horizons. Variations in soil thickness and physicochemical properties have been reported from soil mapping (Erauw, 2019). Due to the complex heterogeneity in the distribution of soil horizons, ash layers, volcanoclastic materials, and lava flows at the transition between toe slope and wetland positions, these soils are not shown in the conceptual diagram (marked with a question mark) since they do not affect the interpretation of the main findings.

Figure 1:

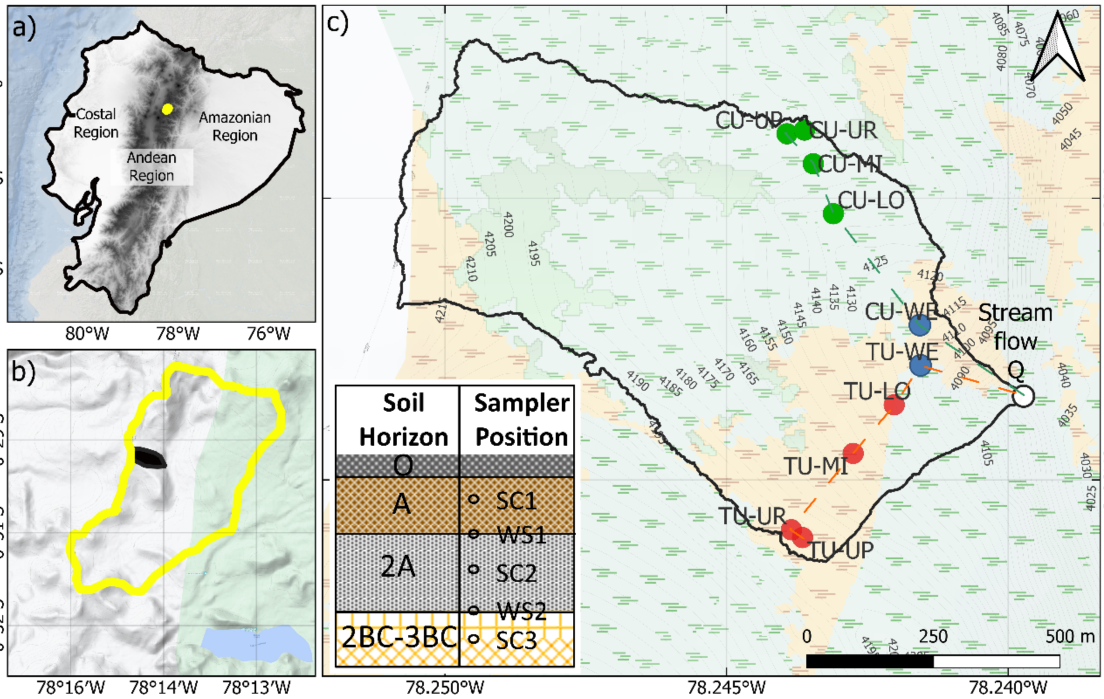
a)
Costal Region
Andean Region
Amazonian Region
0°
2°S
4°S
80°W
78°W
76°W
b)
0°29'S
0°31'S
0°32'S
78°16'W
78°14'W
78°13'W
c)
CU-UP
CU-UR
CU-MI
CU-LO
CU-WE
TU-WE
TU-LO
TU-MI
TU-UR
TU-UP
Stream flow
Q
Soil Horizon
Sampler Position
O
A
2A
2BC-3BC
SC1
WS1
SC2
WS2
SC3
0
250
500 m
0.485°S
0.490°S
78.250°W
78.245°W
78.240°W

Figure 2:

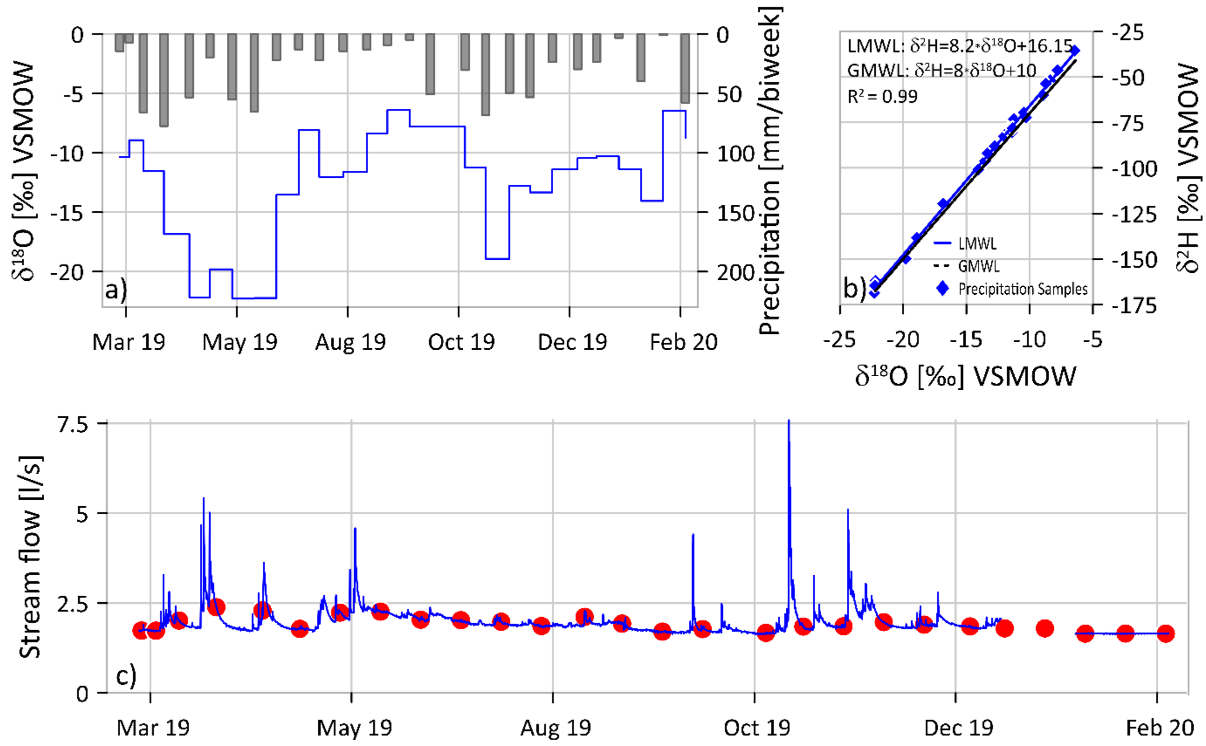

a)
δ18O [‰] VSMOW
Precipitation [mm/biweek]
0
-5
-10
-15
-20
0
50
100
150
200
Mar 19
May 19
Aug 19
Oct 19
Dec 19
Feb 20
b)
LMWL: δ2H=8.2·δ18O+16.15
GMWL: δ2H=8·δ18O+10
R2 = 0.99
LMWL
GMWL
Precipitation Samples
δ18O [‰] VSMOW
δ2H [‰] VSMOW
-25
-20
-15
-10
-5
-25
-50
-75
-100
-125
-150
-175
c)
Stream flow [l/s]
7.5
5
2.5
0
Mar 19
May 19
Aug 19
Oct 19
Dec 19
Feb 20

Figure 3:

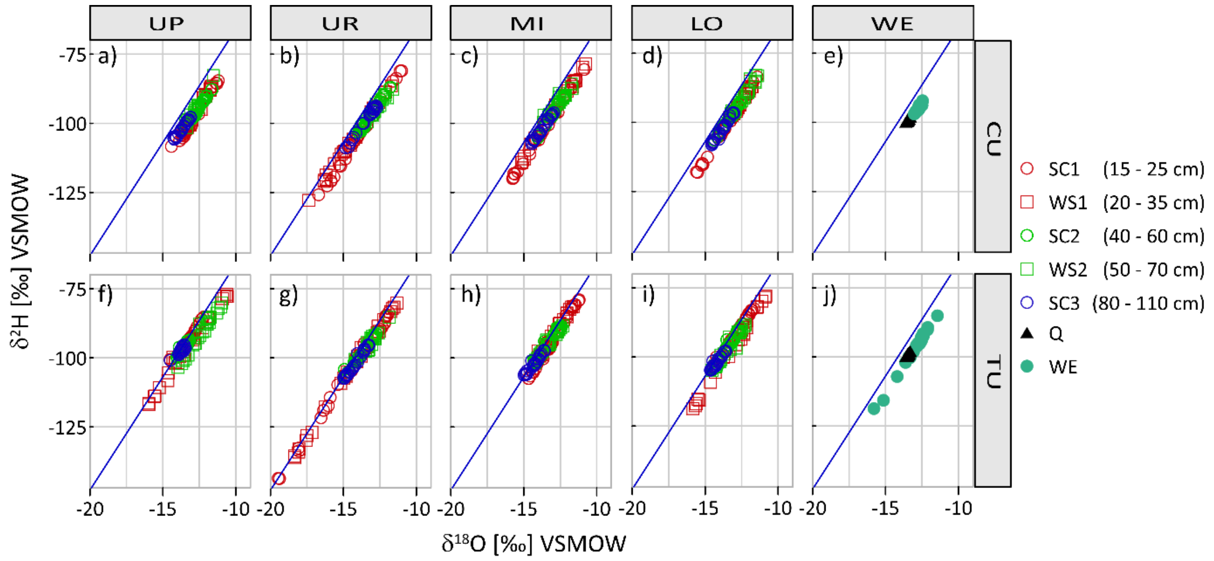
UP
UR
MI
LO
WE
CU
TU
a)
b)
c)
d)
e)
f)
g)
h)
i)
j)
-75
-100
-125
-20
-15
-10
δ²H [‰] VSMOW
δ¹⁸O [‰] VSMOW
SC1 (15 - 25 cm)
WS1 (20 - 35 cm)
SC2 (40 - 60 cm)
WS2 (50 - 70 cm)
SC3 (80 - 110 cm)
Q
WE

Figure 4:

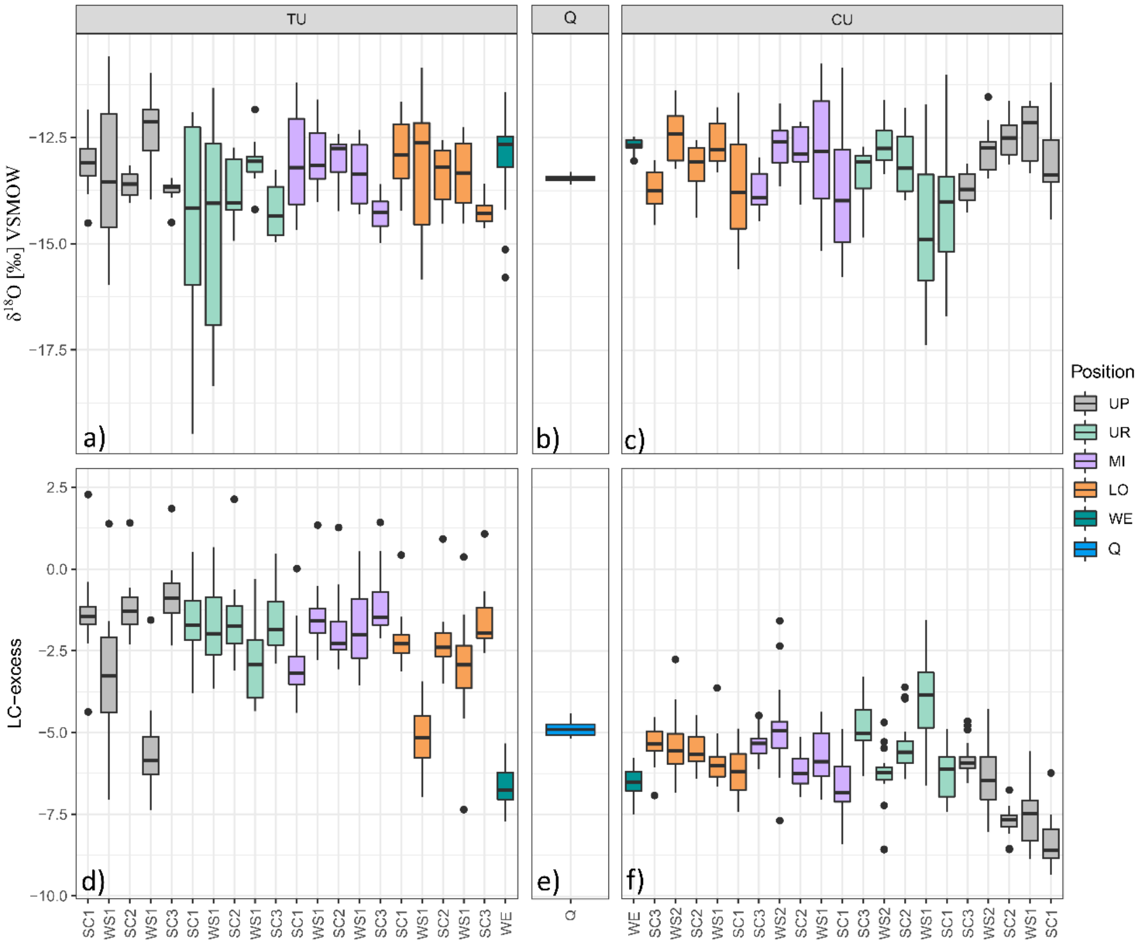
TU
Q
CU
δ18O [‰] VSMOW
−12.5
−15.0
−17.5
a)
b)
c)
LC−excess
2.5
0.0
−2.5
−5.0
−7.5
−10.0
d)
e)
f)
Position
UP
UR
MI
LO
WE
Q

Figure 5:

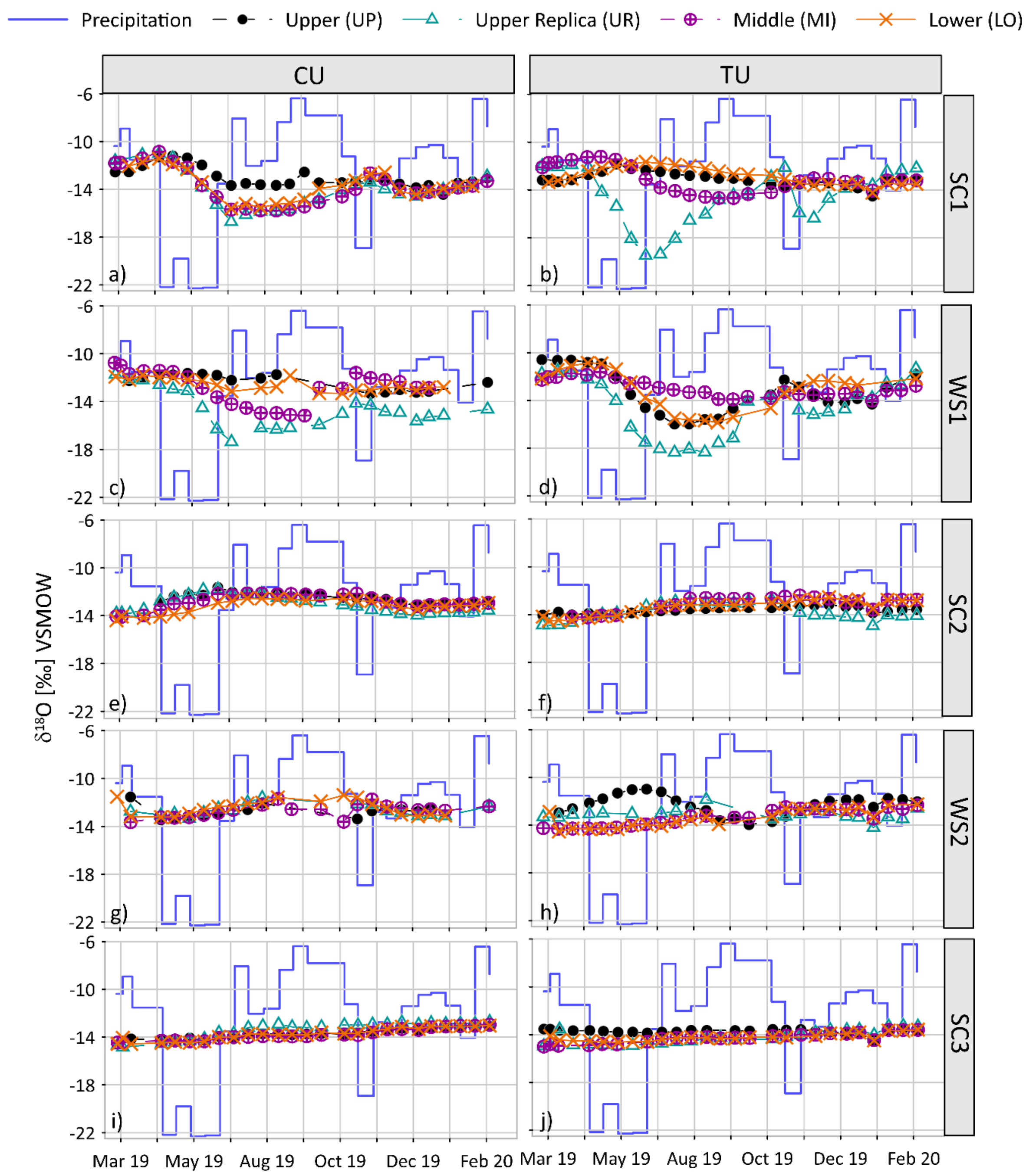

Precipitation
Upper (UP)
Upper Replica (UR)
Middle (MI)
Lower (LO)
CU
TU
SC1
WS1
SC2
WS2
SC3
δ18O [‰] VSMOW
-6
-10
-14
-18
-22
a)
b)
c)
d)
e)
f)
g)
h)
i)
j)
Mar 19
May 19
Aug 19
Oct 19
Dec 19
Feb 20

Figure 6:

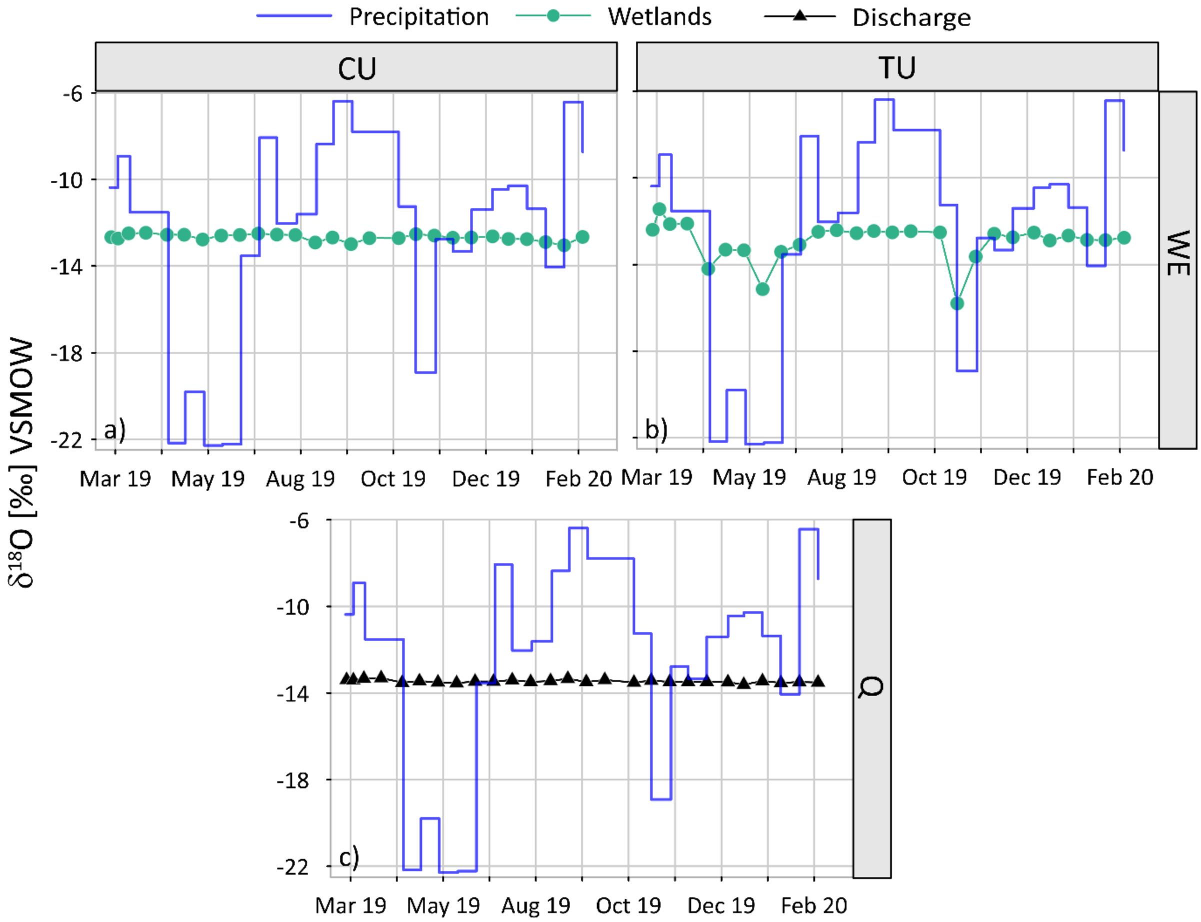

Precipitation
Wetlands
Discharge
CU
TU
WE
Q
δ18O [‰] VSMOW
-6
-10
-14
-18
-22
a)
b)
c)
Mar 19
May 19
Aug 19
Oct 19
Dec 19
Feb 20

Figure 7:

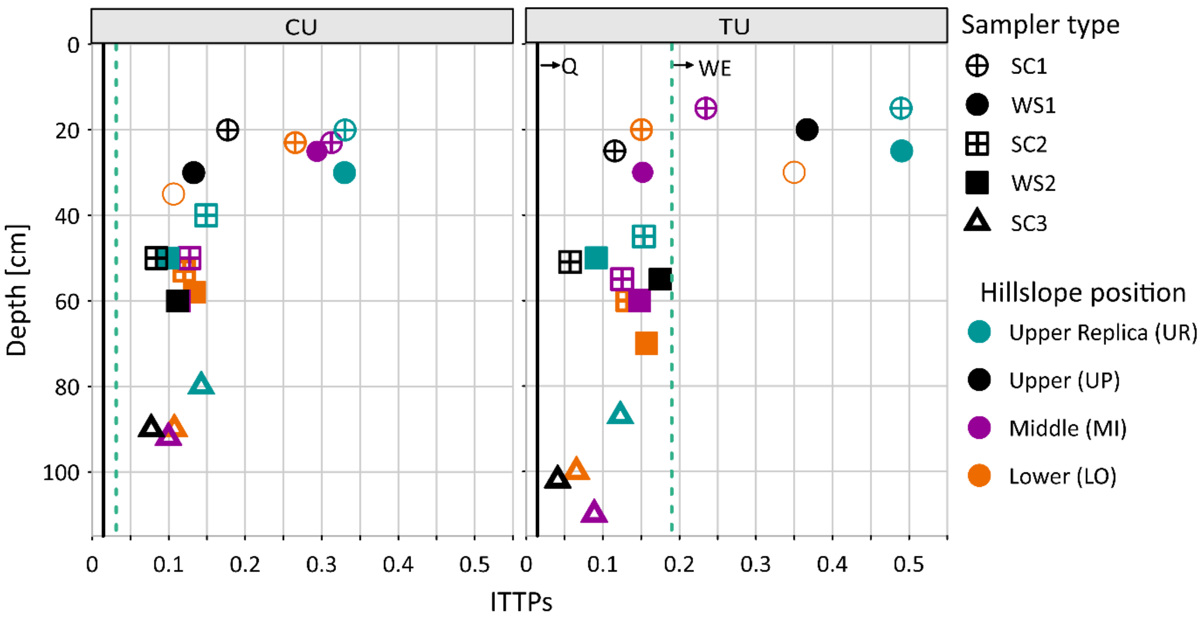

CU
TU
Sampler type
SC1
WS1
SC2
WS2
SC3
Hillslope position
Upper Replica (UR)
Upper (UP)
Middle (MI)
Lower (LO)
Q
WE
Depth [cm]
ITTPs
0
20
40
60
80
100
0
0.1
0.2
0.3
0.4
0.5

Figure 8:

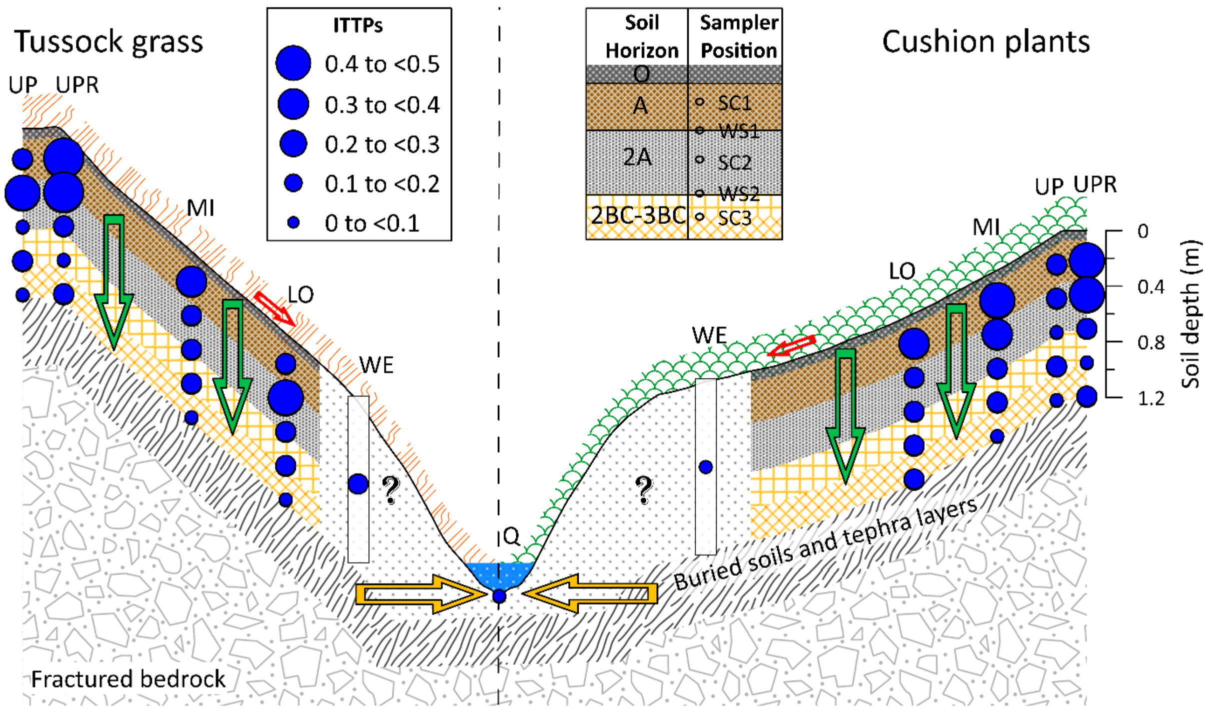

Tussock grass
UP
UPR
MI
LO
WE
ITTPs
0.4 to <0.5
0.3 to <0.4
0.2 to <0.3
0.1 to <0.2
0 to <0.1
Soil Horizon
Sampler Position
O
A
SC1
WS1
2A
SC2
WS2
2BC-3BC
SC3
Cushion plants
UP
UPR
MI
LO
WE
0
0.4
0.8
1.2
Soil depth (m)
?
?
Q
Buried soils and tephra layers
Fractured bedrock